



Aerosol Measurements at South Pole: Climatology and Impact of Local Contamination

Patrick Sheridan^{1*}, Elisabeth Andrews^{1,2}, Lauren Schmeisser^{1,2}, Brian Vasel¹, John Ogren¹

¹ Earth System Research Laboratory, National Oceanic and Atmospheric Administration, 325 Broadway, Boulder, CO 80305, USA

² Cooperative Institute for Research in Environmental Sciences, Boulder, CO 80309, USA

ABSTRACT

The Atmospheric Research Observatory (ARO), part of the National Science Foundation's (NSF's) Amundsen-Scott South Pole Station, is located at one of the cleanest and most remote sites on earth. NOAA has been making atmospheric baseline measurements at South Pole since the mid-1970's. The pristine conditions and high elevation make the South Pole a desirable location for many types of research projects and since the early 2000's there have been multiple construction projects to accommodate both a major station renovation and additional research activities and their personnel. The larger population and increased human activity at the station, located in such close proximity to the global baseline measurements conducted at the ARO, calls into question the potential effects of local contamination of the long-term background measurements. In this work, the long-term wind and aerosol climatologies were updated and analyzed for trends. Winds blow toward the ARO from the Clean Air Sector ~88% of the time and while there is some year-to-year variability in this number, the long-term wind speed and direction measurements at South Pole have not changed appreciably in the last 35 years. Several human activity markers including station population, aircraft flights and fuel usage were used as surrogates for local aerosol emissions; peak human activity (and thus likely local emissions) occurred in the 2006 and 2007 austral summer seasons. The long-term aerosol measurements at ARO do not peak during these seasons, suggesting that the quality control procedures in place to identify and exclude continuous sources of local contamination are working and that the NSF's sector management plan for the Clean Air Sector is effective. No significant trends over time were observed in particle number concentration, aerosol light scattering coefficient, or any aerosol parameter except scattering Ångström exponent, which showed a drop of $\sim 0.02 \text{ yr}^{-1}$ over the 36-year record. The effect of discrete local contamination events in the Clean Air Sector is discussed using one well-documented example.

Keywords: Aerosol monitoring; Clean Air Sector; Wind sector screening.

INTRODUCTION

The National Science Foundation (NSF) operates the Atmospheric Research Observatory (ARO, <http://www.esrl.noaa.gov/gmd/obop/spo/observatory.html>) at its Amundsen-Scott South Pole Station (SPS). The ARO is in a unique location to make global aerosol baseline measurements. Sitting atop the ice sheet of the vast Antarctic Plateau at 2837 m above sea level, the ARO is located typically upwind of the station and thousands of km from any major anthropogenic source regions and permanent human settlements. A Clean Air Sector (CAS, http://www.ats.aq/documents/recatt/Att357_e.pdf) has been defined at ARO,

from which the dominant katabatic winds blow. These downslope winds bring high altitude, free tropospheric air to the station and permit detection of long-range transport of atmospheric trace gases and aerosols to the South Pole. Changes in the atmospheric composition at this location should reflect changes in polar transport pathways or in the southern hemisphere atmospheric background.

The air at the South Pole has long been regarded as some of the cleanest on earth. The National Oceanic and Atmospheric Administration (NOAA) has been making atmospheric measurements of trace gases, aerosols and solar radiation at South Pole since the mid-1970's. Measurements made at the South Pole of atmospheric composition and composition-related parameters by NOAA's Earth System Research Laboratory (ESRL) and its predecessor organizations have typically shown lower values than elsewhere on the planet and are considered global background values (Bodhaine, 1983). Because the concentrations of atmospheric aerosols are typically so low, measurements made at ARO are

* Corresponding author.

Tel.: 1-303-497-6672; Fax: 1-303-497-5590
E-mail address: patrick.sheridan@noaa.gov

particularly susceptible to the possibility of locally-generated aerosols contaminating the baseline measurements. The SPS facilities and infrastructure produce plumes of aerosols in close proximity to one of the most pristine locations on the planet. Activities at SPS that emit particles into the atmosphere (e.g., power generation, aircraft activity, heavy machinery operations, heating, cooking, etc.) could adversely affect the interpretation of the measurements if they are not properly identified as local contamination. The potential for contamination of the background measurements at ARO has been recognized for decades. Hansen *et al.* (1988) used an aethalometer at the South Pole Clean Air Facility (CAF) in 1986 and 1987 and reported ‘black carbon’ (BC) events that greatly exceeded background values when the wind was from the direction of the station. Warren and Clarke (1990) found graphitic carbon in the snowpack downwind of the station with clear indications of the effects of local point sources. Newer aethalometers were deployed both upwind and downwind of the SPS in 1997 (Hansen, 2003b) and concentrations and fluxes of BC from the station were estimated. Concentrations of BC downwind of the station were observed to be as high as $100 \mu\text{g m}^{-3}$, which are 5–6 orders of magnitude higher than the cleanest upwind background values ($0.1\text{--}1 \text{ ng m}^{-3}$).

Fortunately, winds are continuously monitored at the ARO and data are identified as representing either within-CAS or out-of-sector conditions. The extent to which contaminants from the local station environment could enter the CAS and be recirculated back to the ARO after a wind shift has not, to our knowledge, been investigated thoroughly. Hansen (2003b) observed some anomalously high black carbon events at the ARO when winds were from the CAS and suspected local contamination. Some events in the recent data record at ARO permit us to investigate this phenomenon in detail.

Large-scale changes in station activity could alter the frequency of local contamination episodes. Beginning in the late 1990’s, some major changes in station activity occurred at South Pole. Construction began in 1999 on the South Pole Station Modernization (SPSM) project, which included upgrading the fuel storage and power generation facilities and the construction of the new elevated station building. The SPSM project involved the use of heavy machinery for extended periods of time over many austral summer seasons, so diesel engine emissions, welding fumes, etc., in the vicinity of the station were most likely very high relative to non-construction periods. The new elevated station building was ready for conditional occupancy in March 2003 and at that point the number of people that could be accommodated on station at any one time was increased as both the new station and the facilities under the dome were still in operation. SPSM construction activities continued well after 2003 as additional berthing wings of the elevated station building were completed in 2005–2006 and a few other outbuildings (e.g., the cargo/logistics arch) were still being completed as late as 2009.

In the mid-2000’s, two other large research projects took advantage of the increased station capacity. The IceCube Solar Neutrino Observatory (SNO, <https://icecube.wisc.edu/>)

was built between 2004 and 2010, with all construction taking place during the austral summer months of November–February. An array of 86 deep boreholes that reached the Antarctic bedrock was drilled through the ice using a large drilling rig and hot water drill system. Also during this period (austral summers 2005–2007) the 10-m diameter South Pole Telescope was installed. The summertime population at SPS during these years ballooned to maximum capacity due largely to seasonal construction workers and new scientific personnel. In addition to increased emissions by heavy machinery into the local environment, the SPSM and new research projects required many extra LC-130 cargo flights to the Pole to ferry additional personnel, food, fuel, construction materials, and miscellaneous supplies for the workers.

Several recent studies have analyzed NOAA South Pole aerosol data for trends and variability over different time periods. Hereafter in this report, the term ‘SPO’ (NOAA’s South Pole Observatory station) is used to denote the suite of NOAA instruments making atmospheric measurements at the SPS (initially at the South Pole CAF and currently residing in the ARO). The data reported from these instruments are referred to as SPO data, for consistency with previously published results.

Yu *et al.* (2012) reported a downward trend in SPO particle number concentration for the period 1989–2011 and discussed the implications of a warming atmosphere on aerosol nucleation rates and global number concentrations of condensation nuclei (CN) and cloud CN (CCN). Asmi *et al.* (2013) observed a small increasing trend in particle number concentration at the SPO for the most recent decade (2001–2010, inclusive), but slightly decreasing trends in the long term (1974–1988 and 1989–2011). Fiebig *et al.* (2014) used aerosol data from SPO and other Antarctic stations to demonstrate Antarctic-wide annual aerosol cycles. They also noted a small upward trend in SPO particle number concentrations for the period 2007–2011. The results from these studies were likely influenced by a change in the sampling inlet configuration (discussed below) in early 2008 that increased the transmission efficiency of particles into the particle counting instruments, with the maximum impact felt in the Fiebig *et al.* (2014) study due to its shorter time series. No trends in the long-term aerosol light scattering coefficient data over the period 1979–2011 were observed by Collaud Coen *et al.* (2013).

The purpose of this paper is to update the published wind and aerosol climatologies at SPO through 2014 and to evaluate long-term trends in the expanded aerosol data set, including trends in aerosol properties that were not evaluated in previous trend analysis studies. A second question is whether local contamination from human activities has had a noticeable effect on atmospheric measurements at the South Pole, thus, allowing determination of whether any observed changes could be due to local influence or are real trends in the global background aerosol. Station records such as aircraft flight logs, station population numbers, fuel use records and personal notes of station activity are used to gauge human activity and identify potential periods of local contamination at SPO and to relate atmospheric

measurements to overall amount of human activity. The methodology by which discrete contamination events are identified is discussed, and a well-documented example of how these events are handled in the data quality control is presented.

METHODS

Site Description and Meteorology

Atmospheric measurements at ARO are made in some of the cleanest air on the planet, but the Observatory is occasionally impacted by winds from outside the CAS. Fig. 1 shows a diagram of the South Pole research station. By convention at SPS, the Greenwich Meridian (0° longitude) is assigned a grid direction of N (grid 360°), and all directions referenced in this report are relative to the grid. The CAF was used until 1997 and was ~250 m upwind of the Dome. The ARO, which became operational in January 1997, was located an additional ~180 m upwind from the CAF to get farther away from SPS emissions (CMDL, 1998). The ARO sits at the edge of the wedge-shaped CAS, currently defined as lying between grid 340°–110° and extending out to 88° 40' S latitude (~150 km NE of the station). The katabatic

winds typically blow from the NE quadrant, with the highest wind speeds generally from the NNE. The vast majority of human activities occur outside (i.e., downwind) of the CAS. The aircraft flight path crosses over the CAS approximately 1 km NNW of the ARO, but the aircraft are airborne at that point and (usually) turning away from the CAS after take-off. Possible sources of local contamination include the elevated station building, the power plant, aircraft operations, activities associated with the IceCube SNO, motorized vehicles and construction equipment, and other activities. Of these, the largest persistent source of local pollution is power generation from the main station power plant.

A full suite of meteorological measurements are collected at SPO. Wind speed (WS) and wind direction (WD), in particular, are important for determining whether sampled air has come from within the CAS or could have been contaminated by local emissions. The original SPO wind detection system at the CAF was an Aerovane Model 141 system (Bendix, Inc., Baltimore MD), situated on an adjacent tower at ~10 m above the snow surface (CMDL, 1992). This system logged analog signals and recorded 10-min averages of WS and WD signals. This system was replaced in January 1994 by newer and more rugged technology (Model

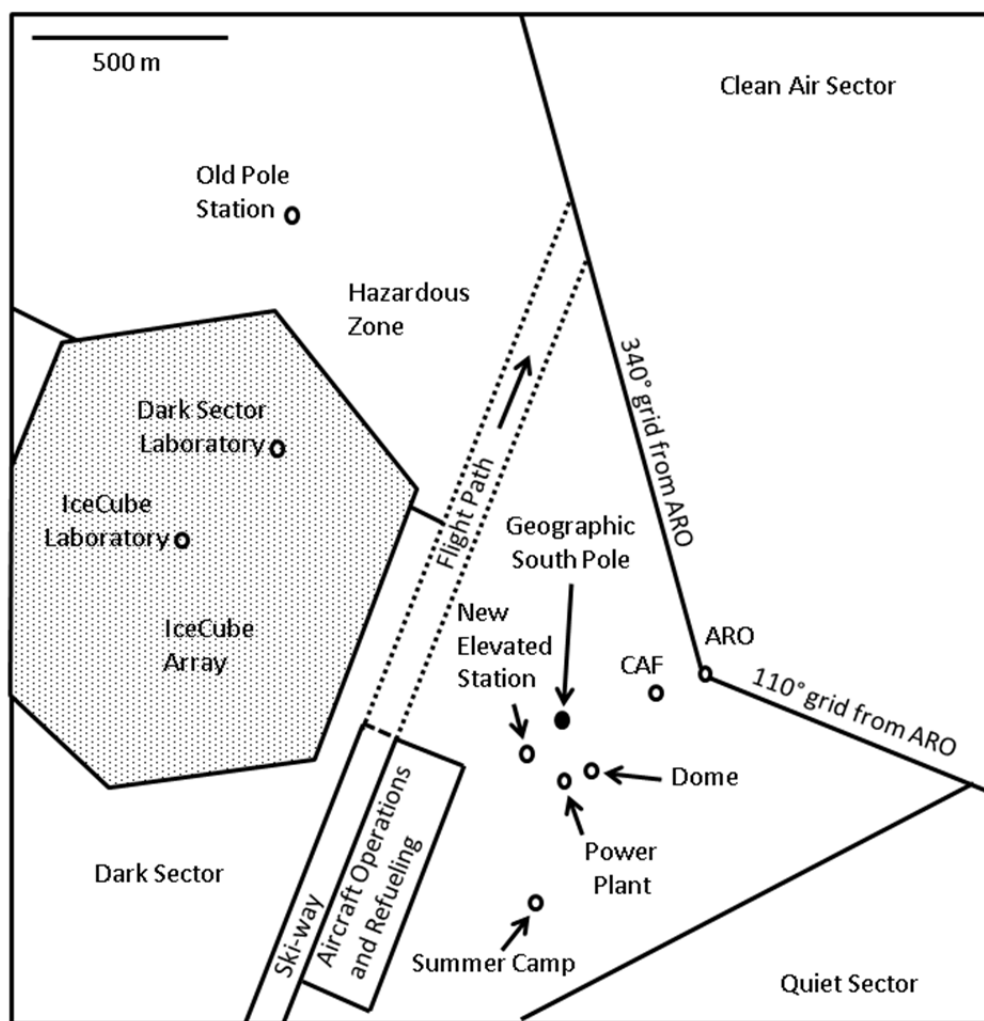


Fig. 1. Map of South Pole Station.

05105, R.M. Young and Co., Traverse City, MI) to better withstand the difficult operating conditions at SPO (CMDL, 1994). At this time the data acquisition system was upgraded and the meteorological measurement recording rate was changed from 10-min to 1-min resolution. In anticipation of the new ARO facility, the SPO meteorological measurements were moved to a new tower near the future laboratory in November 1995. The wind sensors (Model 05103, R.M. Young and Co.) were placed on the tower at a height of 10 m above the snow surface to maintain consistency with World Meteorological Organization/Global Atmosphere Watch (WMO/GAW) sampling protocols. The entire suite of NOAA measurements was moved to the ARO in January 1997 in time for the building dedication.

When winds at ARO are from outside the CAS, or when WS is below a threshold value ($\leq 0.5 \text{ m s}^{-1}$, calm conditions), flags are set in the SPO aerosol data files and these potentially contaminated data are excluded from the ‘clean’ averaged data archives. These data screening techniques based on wind conditions are quite similar to those used in earlier studies at SPO (e.g., Bodhaine, 1995).

Aerosol Measurements

Measurements of the total particle number concentration in atmospheric aerosols began at the South Pole in 1974 (Bodhaine, 1983). A water-based condensation particle counter (CPC), which was a specially-modified General Electric Model 112L428G1 (as described in Bodhaine and Murphy (1980) and Bodhaine, (1983)), operated at SPS for nearly 15 years. At the beginning of January 1989, this instrument was replaced by a newer CPC (Model 3760, TSI Inc., St. Paul, MN) that used 1-butanol as the working fluid. Instrument differences caused an obvious step change in the data series at the start of 1989. This will be discussed more fully in the Results section. Particle number concentration measurements before 1989 were not used in the long term trend analyses. Portions of the SPO particle number concentration data record have been previously reported by Bodhaine (1983) (1974–1981), Bodhaine *et al.* (1986) (1974–1984), Yu *et al.* (2012) (1989–2011), Asmi *et al.* (2013) (1974–2010), and Fiebig *et al.* (2014) (2007–2011).

Based on our calculations, very small particles ($< \sim 40 \text{ nm}$ diam) could be lost by diffusion to the tubing walls of the original SPO CPC sampling inlet at the ARO. Since there were no particle size measurements at ARO, we could not determine the magnitude of the potential particle loss problem. We therefore decided to operate a second CPC system in parallel with the first with a significantly higher flow rate in an essentially identical inlet tube to see if particle losses were lower. In November 2007 a second TSI Model 3760 CPC was installed in the SPO aerosol system. A 0.70-cm inner diameter (ID) conductive metal sampling line, identical to the existing CPC sampling line, was added to the aerosol sampling manifold. The only difference between the two particle counting systems run in parallel was that the new sampling line had a higher flow rate than the old line. In the earlier system a volumetric flow rate of $\sim 1.5 \text{ L min}^{-1}$ was used in the $\sim 3 \text{ m}$ long sampling line. A flow rate of $8\text{--}10 \text{ L min}^{-1}$ was maintained through the inlet line of the

second system and the new CPC extracted 1.5 L min^{-1} from this line. Atmospheric particle concentration measurements were made with the two instruments operating in parallel over the next year (~ 400 day overlap period) and the relationship between the two systems was determined. CPCs were switched on the two inlet lines to determine instrument differences and these were taken into account in the comparisons. The high-speed inlet system appears to measure particle concentrations that are $\sim 6\%$ higher than the low-speed inlet, which can be explained theoretically by lower diffusional losses of small particles in the inlet tubing. This new higher-flow inlet could explain some or all of the small upward trend in the particle number concentrations at SPO observed in recent years by Asmi *et al.* (2013) and Fiebig *et al.* (2014). The low-speed inlet system was taken out of service in February 2009 and the high-speed configuration has been used from that time onward.

CPC instrument performance is checked in several ways. Counter performance is checked periodically by comparison with a trusted NOAA laboratory reference counter that has itself been carefully calibrated. Unfortunately this check can not be performed frequently because of the limitations in getting people and equipment to South Pole. For most of the data record (until end of 2011), daily checks were made with a Pollak photoelectric particle counter (BGI, Inc., Waltham, MA) (Pollak and Metnieks, 1960; Sinclair, 2007) at SPO as reported in Bodhaine (1983). While the Pollak checks are not true calibrations, they can help to spot problems with the continuous measurements. Weekly flow rate checks with a piston-type primary gas flow standard have been instituted in recent years. Relative uncertainties in CPC number concentration measurements have been determined using aerosol electrometers and have been reported in the literature to be around 5% (Fletcher *et al.*, 2009), but with substantially larger uncertainties at the low particle concentrations typically observed at the South Pole.

An integrating nephelometer was installed in 1979 and used to measure the aerosol light scattering coefficient, σ_{sp} , at four wavelengths (450, 550, 700, 850 nm). This nephelometer (Meteorology Research Inc. (MRI), Altadena, CA) was used until its failure in 2002, and a new instrument (Model 3563, TSI Inc., St. Paul, MN) replaced it in November 2002. The TSI nephelometer was developed from the MRI instrument, using three of the same wavelengths (450, 550, 700 nm) and a similar optical geometry, so the same corrections are applied to both sets of data. A period of parallel operation was not possible for the two nephelometers at SPO due to the failure of the MRI instrument, but a 1-yr overlap comparison between the same nephelometer models was done at the NOAA Baseline Observatory at Barrow, Alaska and showed agreement for σ_{sp} at 550 nm to within 1%. The TSI nephelometer has a backscatter shutter that is rotated into place for measuring scattering over the angular range of $90^\circ\text{--}170^\circ$. From this measurement of the hemispheric backscattering coefficient (σ_{bsp}), and the total scattering coefficient, an estimate of the hemispheric backscatter fraction (b), is made. Table 1 lists the deployment time range and the measured and derived quantities from each nephelometer.

Table 1. Atmospheric aerosol light scattering determinations made at SPO using the MRI and TSI nephelometers.

	Parameter or Equation	MRI Nephelometer	TSI Nephelometer
Deployment Period		Feb 1979–Nov 2002	Nov 2002–present
Wavelengths (nm)		450, 550, 700, 850	450, 550, 700
Scattering Coefficient	σ_{sp}	Yes	Yes
Hemispheric Backscatter Coefficient	σ_{bsp}	No	Yes
Scattering Ångström Exponent	$\hat{a}_s = -\log[\sigma_{sp(550nm)}/\sigma_{sp(700nm)}]/\log[550/700]$	Yes	Yes
Backscatter Fraction	$b = \sigma_{bsp(550nm)}/\sigma_{sp(550nm)}$	No	Yes

The nephelometer data are corrected for angular nonidealities using the size-dependent correction scheme of Anderson and Ogren (1998). The same nephelometer correction methods are employed at all NOAA atmospheric monitoring locations. Frequent calibration and background checks of the SPO nephelometer are necessary to accurately measure the low scattering coefficients at South Pole and are conducted using standard NOAA and WMO/GAW protocols. Nephelometer backgrounds are determined every 30 minutes at SPO, and calibration checks are performed bi-monthly to see if the instrument calibrations have drifted. If the calibrations are found to have drifted outside of an acceptable range (~5%), the nephelometer is recalibrated. A Nephelometer Operation Manual is available that provides more information on the calibration checks, recommended instrument settings, maintenance schedules, troubleshooting hints, etc., at <http://www.esrl.noaa.gov/gmd/aero/docs/index.html>.

Relative uncertainties in the light scattering coefficients made by TSI nephelometers have been reported previously. Sheridan *et al.* (2001) reported a total analytical uncertainty from all sources for 1-min average TSI nephelometer σ_{sp} data (550 nm wavelength) of around 10% for a scattering level of 33 Mm⁻¹. In a more detailed analysis, Sherman *et al.* (2015) reported relative measurement uncertainties for different averaging times and different scattering ranges, and reported a total relative uncertainty of ~10% for hourly-average σ_{sp} data (550 nm) at a scattering level of 1 Mm⁻¹. Portions of the SPO record of aerosol light scattering coefficients have been published by Bodhaine (1983) (years 1979 and 1981), Bodhaine *et al.* (1986) (years 1979 and 1981–1984), Bodhaine (1995) (year 1987), and Collaud Coen *et al.* (2013) (years 2003–2010).

Aethalometers (Magee Scientific Co., Berkeley, CA) were used on an intermittent basis at the South Pole to determine equivalent black carbon (EBC) concentration. Since the aethalometer instrument actually makes a light absorption measurement, we are following the recommendations of Petzold *et al.* (2013) by reporting in Table 2 the wavelengths and specific absorption constants (i.e., Sigma(BC) values) used by each instrument to convert the light absorption measurements into EBC mass concentrations. Portions of the South Pole aethalometer data record have been previously reported by Hansen *et al.* (1988), Bodhaine (1995), and Hansen (2003b). One deployment lasted from 1987–1990 and used an instrument (Model AE-8) with an incandescent light source and a broadband detector. This early broadband instrument showed a spectral response for elemental carbon particles on the aethalometer filter peaking at 830 nm and

used a Sigma(BC) of 19 m² g⁻¹ for the determination of EBC concentration (Bodhaine, 1995). Weingartner *et al.* (2003) determined the spectral response of a similar aethalometer with the same broadband source (Model AE-10) on exposed filters to be ~840 nm. Another deployment, using an instrument with a solid state light source operating at 880 nm (Model AE-16) lasted for most of 1997. The aethalometer manual (Hansen, 2003a) states that the Model AE-16 uses a Sigma(BC) value of 16.6 m² g⁻¹ to calculate its reported EBC concentrations. A seven-wavelength aethalometer (Model AE-31) was installed and has been operating continuously at SPO since January 2006. The AE-31 EBC concentrations reported here are derived from the 880 nm wavelength channel using the same Sigma(BC) value of 16.6 m² g⁻¹ (Hansen, 2003a). The EBC data record from South Pole is clearly intermittent and the degree to which comparisons can be made between the different aethalometer models unknown, but all of the data have been included here for completeness. It is widely recognized that aethalometer data overestimate absorption values, and various correction schemes exist to account for this (Collaud Coen *et al.*, 2010, and references therein). Since this study does not compare the South Pole aethalometer measurements to other concurrent absorption measurements or absorption values from other locations, a correction is not applied to the data. Although the authors recognize the importance of this correction for some applications, it is not deemed necessary here for the EBC trend analysis.

RESULTS AND DISCUSSION

Wind Climatology

An updated wind climatology for SPO for the years 1979–2014 using hourly-average wind data is shown in Fig. 2. If mean WS ≤ 0.5 m s⁻¹ (calm conditions), then the 1-h wind data were not included. The percentage of hours the wind blew from each five-degree sector is shown by the length of each wedge and the relative amount of time for each wind speed range is also shown. As a check, the same analysis was performed for two years (2013 and 2014) using 1-min resolution wind data. For 2013, the percentage of observations spent in the CAS based on 1-h data was 88.46% and based on 1-min data was 88.63%. For 2014, the percentage of observations spent in CAS based on 1-h data was 89.49% and, based on 1-min data, was 89.39%. The small climatological differences in the fraction of wind observations coming from the CAS between 1-min and 1-h data are most likely due to our vector averaging methods and round off errors. This indicates that for SPO there is

Table 2. Aethalometers used at SPO¹ and their operating parameters.

	AE-8	AE-16	AE-31
Period of Observations	Jan 1987–Dec 1990	Feb–Nov 1997	Jan 2006–present
Wavelengths (nm)	Broadband ²	880	880
Sigma(BC) (m ² g ⁻¹)	19.0	16.6	16.6

¹ A Model AE-33 aethalometer has been in continuous operation at SPO since April 2013.

² Spectral response peak at 830 nm.

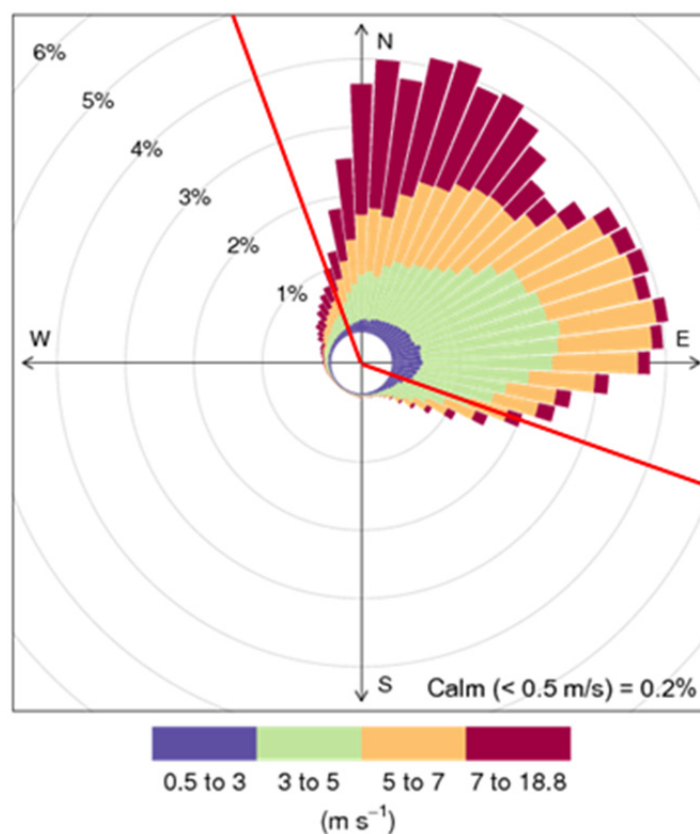


Fig. 2. Wind rose of hourly-average SPO winds for the years 1979–2014. Hours for which wind speed was $\leq 0.5 \text{ m s}^{-1}$ were excluded from the analysis. Wedges represent five-degree directional sectors from which the winds blow, and the red lines show the boundaries of the CAS.

essentially no difference between using 1-h and 1-min wind data to construct the wind climatology. Additional information on the CAS and yearly wind rose plots for SPO are available at <http://www.esrl.noaa.gov/gmd/obop/spo/observatory.html>.

The fraction of time winds blow from the CAS varies from year to year. Fig. 3(a) shows this statistic for each year since 1979. The various traces represent different thresholds for acceptance of winds of sufficient velocity, with the one used in this study ($WS > 0.5 \text{ m s}^{-1}$) shown with a bold red line. This plot shows that the choice of the calm wind rejection threshold does not appreciably affect the results, because the WS at SPO is typically much larger than 2 m s^{-1} . The mean value of winds from the CAS over all years is $\sim 88\%$, and there is substantial year-to-year variability in this number. The variability in the yearly fraction of wind observations from the CAS appears to have increased after 1991. A two-sample t-test was performed

on the $WS > 0.5 \text{ m s}^{-1}$ data series to compare the means from 1979–1991 and 1992–2014. The means of the yearly CAS fractions were 88.3% and 87.5% for the 1979–1991 and 1992–2014 periods, respectively. These means are not statistically different at a confidence level of 95% ($p\text{-value} = 0.19$). The variability observed in this data set is not related to any instrument or sampling location changes and appears to be most closely associated with winds near the CAS boundary at grid direction 110° . The yearly wind rose plots at <http://www.esrl.noaa.gov/gmd/obop/spo/observatory.html> show that most of the out-of-sector winds lie to the southeast of grid direction 110° . As an example, the year 2002 shows a large bulge in the fraction of WD observations in the $110^\circ\text{--}135^\circ$ directions, and 2002 is one of the years in the record with the largest fraction of out-of-sector winds.

Fig. 3(b) shows how these results would change if the slightly larger historical CAS definition of grid $330^\circ\text{--}110^\circ$ (as was reported in Bodhaine (1995) and earlier papers)

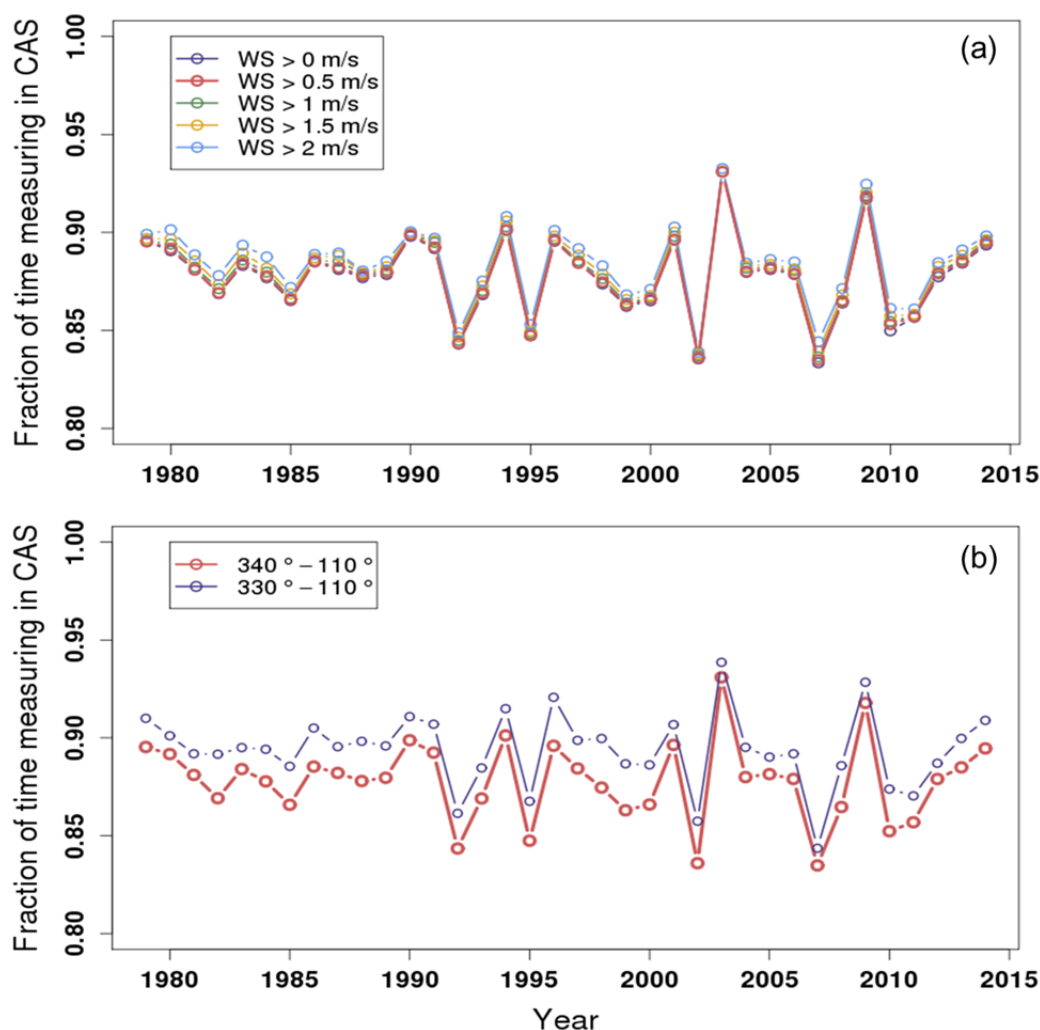


Fig. 3. Fraction of total hours each year (1979–2014) winds were from the CAS (a) showing small differences based on the calm wind rejection threshold, and (b) showing the comparison with the historical definition of a slightly larger CAS.

was used. The mean, median and standard deviation (S.D.) of measurements from the two different sectors is presented in Table 3. We find that the winds measured at ARO blow from the CAS about 88% of the time, and even with the wider CAS used in earlier studies we observe the winds to be from the CAS ~89.5% of the time. This is not consistent with earlier reports of winds at SPO coming from the CAS > 98% of the time (covering the years 1977–1983; Bodhaine et al. (1986)) or ~95% of the time (covering the years 1987–1990; Bodhaine (1995)). The details of the data screening methods used in the earlier studies are not known, but for the current analysis, if a 1-h average wind value lies

Table 3. Fraction of all SPO hourly observations with CAS winds.

Fraction in CAS	Mean	Median	S.D.
<i>CAS definition</i>			
340°–110° (this study)	0.878	0.880	0.021
330°–110° *	0.894	0.895	0.019

* (CAS as defined in Bodhaine et al., 1995) and earlier papers.

outside of the CAS, it is treated as out of sector. Using this method, our data from these periods do not support the notion of CAS winds blowing 95% of the time.

Long term time series (1980 through 2014) of WD and WS are shown in Fig. 4. Monthly means of WD are plotted in Fig. 4(a) and the envelope of the monthly standard deviations (based on 1-h data) is shown in gold. Winds from the northeast (i.e., CAS) dominate as expected. One month showed mean winds from the north (Jan 1998, 357°), which stands out on the plot because of the plotting method but is still well within the CAS (grid 340°–110°). The monthly variability of the WD record is shown in the inset box. The box-whiskers plots in this and other figures in this paper show monthly medians (horizontal bar in box), quartiles (ends of box), and 5th/95th percentiles (ends of whiskers) of the distributions. Winds are northeasterly for most of the year and turn a little more northerly during the austral summer. Fig. 4(b) shows the WS time series plotted in the same way. Monthly mean wind speeds at SPO are fairly consistent over most of the year but drop to lower values during the austral summer months of December, January and February. These data show essentially no trend over

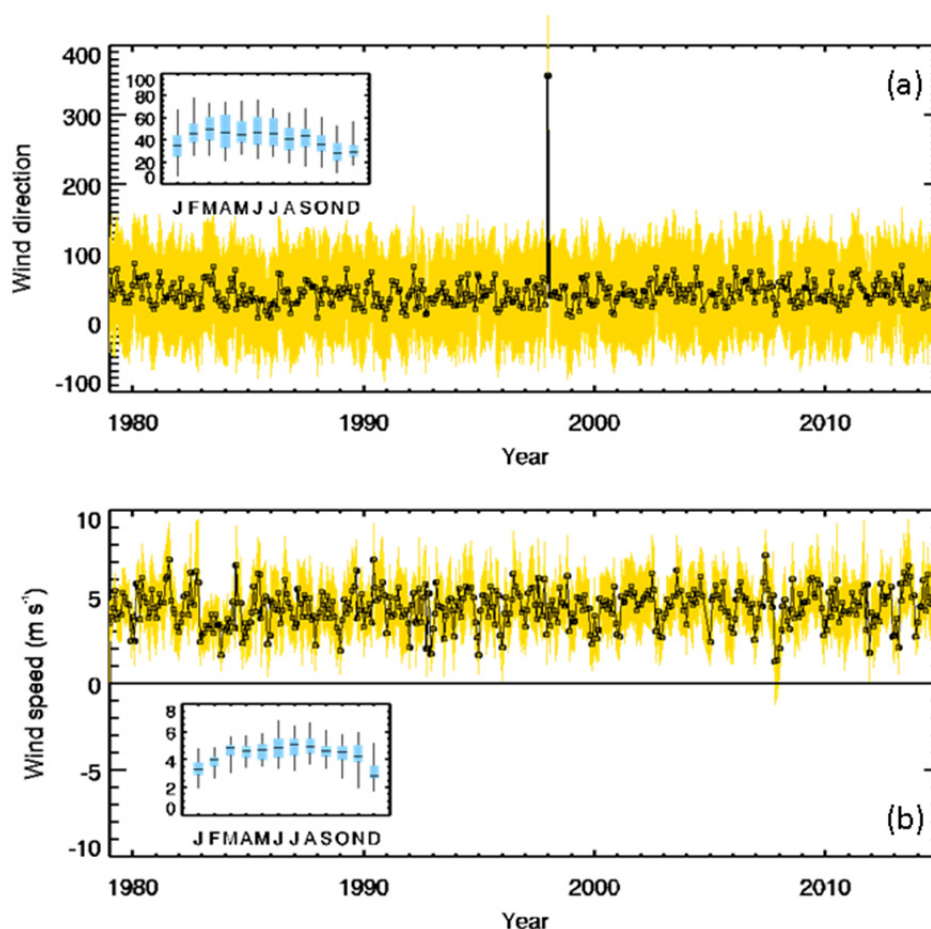


Fig. 4. Time series plots of (a) mean monthly wind direction and (b) mean monthly wind speed. Standard deviations of the monthly mean values are shown as gold bars, and population statistics (median, quartiles, 5th/95th percentiles) by month are displayed in the inset boxes.

the duration of the 35-year record and do not support the idea of major changes in circulation patterns at South Pole.

Markers of Human Activity at South Pole

The decade of the 2000's saw increasing station population at SPS both because of the construction activities and new science projects. The larger population required more support in the form of food, materials, fuel and other resources. LC-130 aircraft are used as a primary way to move people and resources to and from Pole, and these flights increased accordingly during this time. Presumably more people, flights, fuel use, etc., at SPS would lead to more local particulate emissions, and here we examine whether there is any indication of contamination due to increased activity on the SPO aerosol measurements at the ARO.

Fig. 5 shows these crude markers of human activity at SPS. The numbers of LC-130 flights between McMurdo Station and SPS and the amount of fuel delivered to SPS each year have been supplied by the NSF's Antarctic Support Contractor (ASC, personal communications, 2015). The station population numbers were obtained through logs, notes and records kept at SPS. The convention used in Fig. 5 is that a given year on the graph represents the austral summer period when the station was open that year. For

example, '2015' represents the activity during the 2015 austral summer season, which is November 2014 through February 2015. Winter population, since it represents the period between station closing and opening (approx. February through October), is plotted on the half-year.

All markers show broad peaks in the mid-2000's, with maxima for the individual time series all occurring in the time period of mid-2005 through 2007. Station summer population peaked during the height of the IceCube SNO drilling activity at close to 300 in 2007, and this was also the year of maximum fuel delivered to SPS. A large amount of fuel (second highest annual total) was delivered in the 2008 summer season, meaning that a relatively large amount of fuel was burned at SPS in calendar year 2008. These data suggest that peak activity, and thus aerosol emissions, at the SPS occurred in the summer seasons of 2006–2008, represented by the 'MAX' bar on the figure. Overland traverses of fuel began in the 2012 summer season (November 2011–February 2012). This reduced the amount of fuel brought in by aircraft and the total number of LC-130 flights. For the summer seasons 2012–2015, the lower branch of the red curve shows fuel delivered to SPS by LC-130 aircraft and the upper branch shows the total amount of fuel delivered both by aircraft and overland traverse.

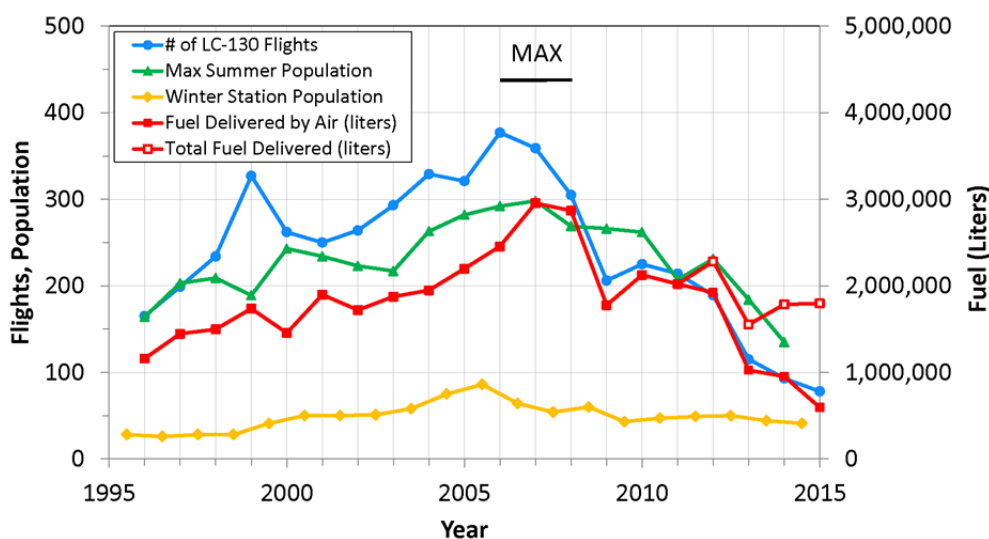


Fig. 5. Markers of human activity at South Pole. The ‘MAX’ bar shows the period of maximum human activity at SPS, and covers the austral summer seasons 2006–2008. The fuel trace splits at the 2012 summer season reflecting the start of fuel delivery via overland traverses. The Total Fuel trace is the sum of fuel delivered by aircraft and surface transport.

Aerosol Climatologies

Time series of monthly averages of the primary aerosol measurements at SPO from the first aerosol measurements in 1974 through the end of 2014 are presented in Fig. 6. The instrument change from the water-based CPC to the butanol-based instrument at the beginning of 1989 is apparent in the particle number concentration plot (Fig. 6(a)). The cause of the step change in the data record is not known conclusively, but could include dissimilarities in the ranges of particle sizes detected, different particle losses upstream of the optics, hydrophilic material in aerosol particles not growing as efficiently in the water-based CPC (Liu *et al.*, 2006; Hermann *et al.*, 2007), and flow calibration issues. These particle counters were not to our knowledge ever run in parallel. A few gaps where instruments failed are also evident. A trend analysis is presented for the most reliable portion of the data record (1989–2014), and a linear least-squares fit of these monthly data is shown as a red line. The open source R package ‘OpenAir’ (Carslaw and Ropkins, 2012; Carslaw, 2015) was used to apply a Mann-Kendall non-parametric approach with bootstrap simulations to determine the Theil-Sen slope and statistical significance of the time series trends of each of the aerosol parameters. The monthly data were deseasonalized and autocorrelation was accounted for. The particle number concentration trend of $-0.2 \text{ cm}^{-3} \text{ yr}^{-1}$ is not significant for the 26-yr time period of the butanol-based CPC. The lack of a significant trend in number concentration differs from results reported in Yu *et al.* (2012) and Asmi *et al.* (2013) who found small decreasing but statistically significant trends (at $p < 0.05$) for the time period 1989–2011. Our data set ends in late 2014 and includes more measurements from the higher-transmission aerosol inlet that was installed in late 2007, so this could weaken the observed downward trend and partially explain this discrepancy.

A clear annual cycle in number concentration is observed in the monthly data. The inset box in Fig. 6(a) shows this

annual cycle (reported for the period of the trend analysis) in more detail. The monthly maximum is in February, with a smaller secondary maximum in November, and relatively high values throughout the austral summer. These results are consistent with the average annual cycle presented in Bodhaine *et al.* (1986), which covered the years 1974–1984 and showed maxima during the same two months (although their November value was slightly larger than their February one). The Antarctic polar vortex typically forms in late March to early April and breaks down in early to mid-November (<https://www.nsf.gov/about/history/nsf0050/arctic/ozone.htm>). The polar vortex is solidly set up over Antarctica during the austral winter months (June–August) when particle number concentration shows its lowest values. This is consistent with the idea of a known loss mechanism (dry deposition to the snow surface) operating in an isolated air mass with little replenishment of particles or condensable gases from long range transport of air masses to Antarctica, and the lack of sunlight at South Pole during winter eliminating photochemical production of particles.

The SPO annual cycle in particle number concentration agrees well with observations at other atmospheric monitoring stations in Antarctica. At Troll Atmospheric Observatory (72.0° S latitude) on the coast of Antarctica, Fiebig *et al.* (2014) attributed the higher summertime values to photooxidation-limited particle production during the sunlit time of the year, and argued that the annual cycle observed at Troll is in fact a widespread phenomenon common to central Antarctic air masses. The annual cycle in particle number concentration at the coastal Neumayer station (70.7° S latitude) shows a similar shape as those at SPO and Troll (Spracklen *et al.*, 2010).

The long-term (36 year) record of monthly average σ_{sp} at 550 nm is presented in Fig. 6(b). The overall trend for the period 1979–2014 (not statistically significant, slope = $0.00 \text{ Mm}^{-1} \text{ yr}^{-1}$) is shown as a red line. The lack of a trend in σ_{sp} at SPO is consistent with the findings of Collaud

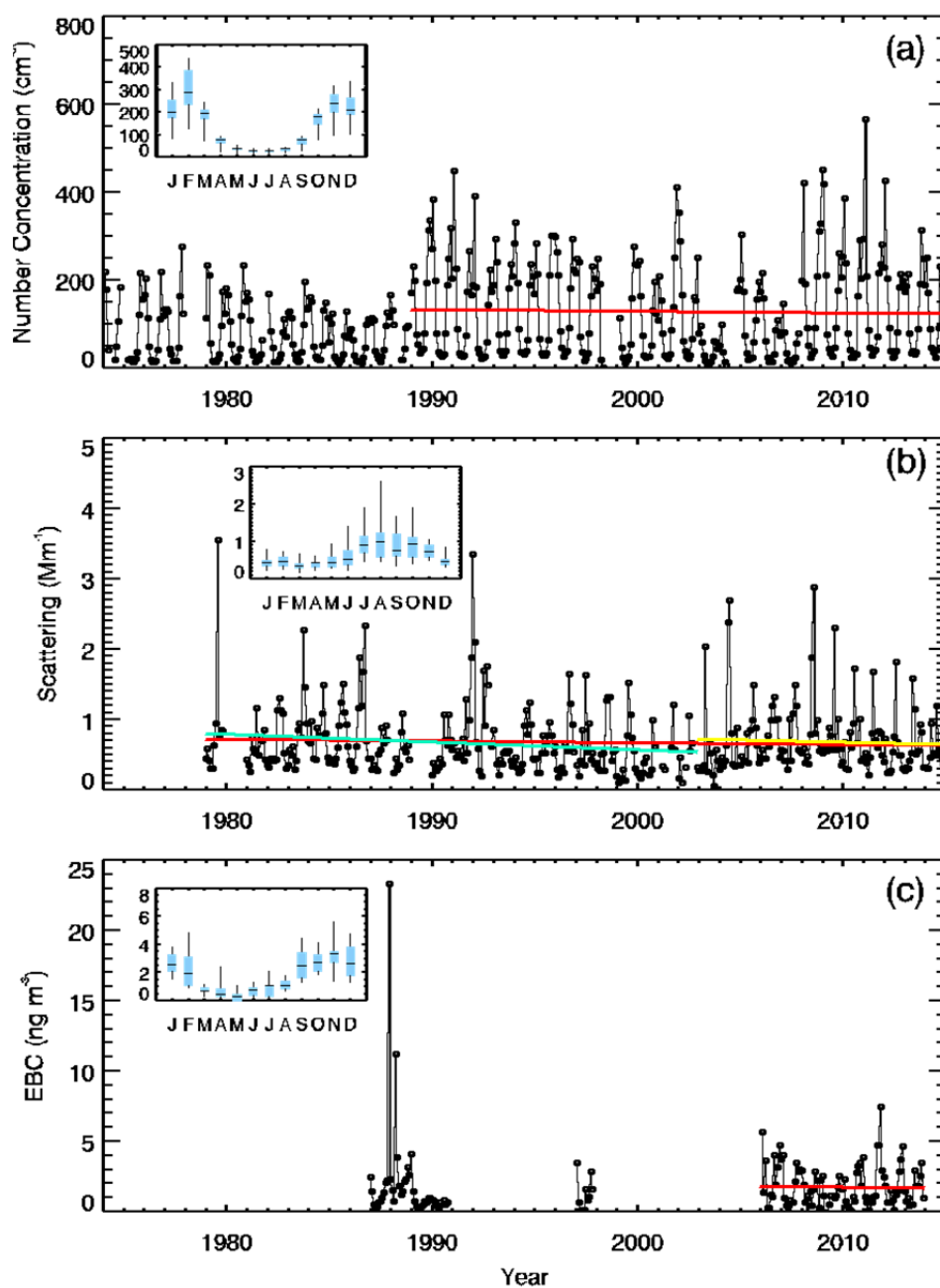


Fig. 6. Time series of primary aerosol measurements at ARO. Linear least-squares fits of the monthly average data points over the most reliable portion of the data records are shown as red lines. (a). Total particle number concentration. (b). Aerosol light scattering coefficient (550 nm wavelength). Green line shows the linear least-squares fit of the 1979–2002 period, while the yellow line shows the fit for the 2002–2014 period. (c). Equivalent black carbon concentration.

Coen *et al.* (2013). Trends were also determined for the σ_{sp} measurements from the two nephelometers separately. The trend 1979–2002 for the MRI nephelometer is shown as a green line and was found to be significant ($p < 0.001$) but with a slope of $-0.01 \text{ Mm}^{-1} \text{ yr}^{-1}$. This is well within the uncertainty of the scattering measurement. The trend for the TSI nephelometer (yellow line) during the 2002–2014 period was not statistically significant (slope = $0.00 \text{ Mm}^{-1} \text{ yr}^{-1}$).

A very different annual cycle is seen for σ_{sp} in Fig. 6(b) than was shown for number concentration. The larger scattering coefficients are observed in the late austral

winter and early austral spring at SPO, with July, August and October showing the highest values. Similar results were reported in Bodhaine *et al.* (1986) (years 1979–1984) and Bodhaine (1995) (year 1987), which showed a broad peak at the same time of year. The September local minimum reported in this study was also observed in both Bodhaine papers. The broad late-winter and spring maximum in σ_{sp} has been attributed to transport of sea salt aerosols from open water coastal areas surrounding the Antarctic continent (Parungo *et al.*, 1981; Harris, 1992; Bodhaine, 1995).

The South Pole record of monthly-average EBC

concentration is presented in Fig. 6(c). No significant trend (slope = $0.0 \text{ ng m}^{-3} \text{ yr}^{-1}$) was observed for the 8 year period that EBC was continuously measured at SPO. To our knowledge, trends for EBC at SPO South Pole have not been previously reported.

The annual cycle of EBC is similar to that of particle number concentration with a broad peak in the austral summer and very low values in the austral winter. This suggests that particle number concentration and EBC at SPO may be controlled by some of the same production or removal processes. We observed a very high monthly EBC value ($\sim 23 \text{ ng m}^{-3}$) in December 1987 and another high point in April 1998 ($\sim 11 \text{ ng m}^{-3}$) for which our screening procedures do not provide any indication of contamination due to wind conditions or particle number concentration. Other than the two months mentioned above, all monthly average EBC values at SPO were $< 8 \text{ ng m}^{-3}$. Bodhaine (1995) published daily-average BC (i.e., EBC) data in their Fig. 5 that appear to show large ($> 30 \text{ ng m}^{-3}$) daily mean BC concentrations in December 1987. The EBC results presented in this paper for the 1987–1990 period use the same aethalometer BC data as Bodhaine (1995), although the screening and analysis methods used could have been different. We can not compare these points quantitatively

with the earlier published results because monthly averages were not presented, but the Bodhaine (1995) daily-average data corroborate the large December 1987 EBC peak in this study.

Monthly-average values of the intensive aerosol properties \hat{a}_s and b are plotted in Fig. 7. The \hat{a}_s data from the two integrating nephelometers operating at the same wavelengths are shown in Fig. 7(a). Backscatter fraction data, available only from the newer nephelometer installed in late 2002, are shown in Fig. 7(b). Annual cycles of \hat{a}_s and b are similar with higher values (suggesting a larger contribution to light scattering from smaller particles) observed in the austral summer months. This supports the earlier findings of sea salt aerosols (i.e., larger particles) having a greater impact at South Pole during late winter and spring.

The monthly average values for \hat{a}_s in Fig. 7(a) show a linear slope of $\sim -0.02 \text{ yr}^{-1}$ over the period 1979–2014. Using the same Mann-Kendall trend analysis package described above, we find that the trend (Theil-Sen slope) for \hat{a}_s is also -0.02 yr^{-1} and statistically significant at the $p < 0.001$ level (i.e., highly significant), although the slopes for the pre-2002 and post-2002 scattering measurements (green and yellow trend lines, respectively) were each found to be not significant. The mean \hat{a}_s of the post-2002 period (1.39

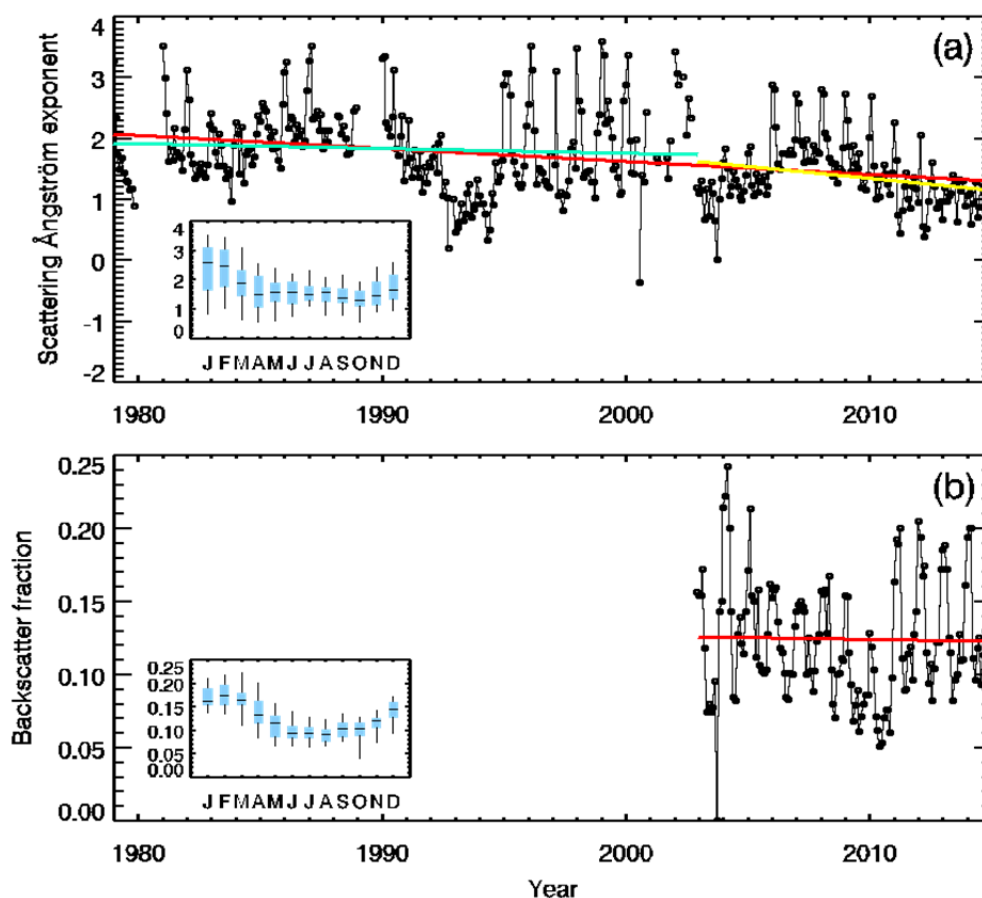


Fig. 7. Time series of aerosol intensive properties at ARO. Linear least-squares fits of the monthly average data points are shown as red lines. (a). Scattering Ångström exponent (550/700 nm). Green line shows the linear least-squares fit of the 1979–2002 period, while the yellow line shows the fit for the 2002–2014 period. (b). Hemispheric backscatter fraction (550 nm).

± 0.52 S.D.) is lower than that of the pre-2002 period (1.83 ± 0.70 S.D.). Since the older nephelometer failed and the instruments could not be run in parallel for an overlap comparison, we have no way of knowing if the older instrument had a problem with its red channel. If it did this could influence the comparison of the green-red \hat{a}_s for the two periods.

The 14-year trend for b (0.00 yr^{-1}) in Fig. 7(b) is not statistically significant. The b does not show the same downward trend (toward larger particles) as the \hat{a}_s , and this may be because b is most sensitive to a different part of the particle size distribution than is \hat{a}_s (550/700 nm) and have frequently been found to not track each other closely (e.g., Collaud Coen *et al.*, 2007). It is possible that a long term change in the aerosol composition and/or size distribution has occurred at SPO over the measurement period, but there are no long-term aerosol chemical or microphysical measurements at South Pole to corroborate this possibility. As mentioned above it is also possible that the nephelometer instrument change in 2002 affected this \hat{a}_s measurement to some extent. The \hat{a}_s values since 2002 tend to be slightly lower than for the earlier years, and this would certainly affect the trend.

Effect of Local Emissions on the Long Term Aerosol Record

There are no historical emissions inventories at SPS so we cannot know for sure when in the historical record local aerosol emissions peaked and what the magnitude of those emissions were. We believe, however, that the markers of human activity presented in Fig. 5 serve as proxies for anthropogenic pollution at South Pole and thus track local aerosol emissions. The wind data presented in Figs. 2, 3 and 4 suggest that (1) a significant number of hours, $\sim 12\%$ of the total sampling time, is spent sampling air from outside the CAS, and (2) this wind scenario at SPO has not changed appreciably since 1980. Aerosol data are automatically flagged as contaminated when winds are calm or blow from directions that fall outside of the CAS, so local station emissions are typically caught by the WD or WS flagging criteria. The problem occurs when winds blow local emissions past the ARO and out into the CAS where the aerosols can linger because of the lack of wet removal processes or be deposited on the snow surface. If a wind shift then occurs these locally-generated aerosols can be recirculated back to ARO and be directly sampled, or the particulate material attached to the surface snow/ice crystals can be re-entrained and brought into the ARO inlet where the crystals are evaporated, leaving the particles. In either case the aerosol data would be interpreted as clean background

data based on wind direction alone. Hansen (2003b) observed several instances during an aethalometer study in 1997 where high BC values were observed when the wind was from a direction well within the CAS and concluded that these incidents were local contamination events. The current NOAA quality control protocol for SPO has several criteria based on wind and particle number concentration measurements for identifying likely contamination events and these are reported in Table 4. A scattering coefficient criterion has not been used because it often does not respond to fine particle events as might be present when local aircraft or power plant effluents impact the site. The aethalometer EBC data are intermittent throughout the record and were not used to determine contamination events.

The WD and WS filters catch almost all of the local contamination events ($\sim 93\%$). In cases where a wind shift brings locally-generated aerosols back out of the CAS to the ARO, two other automatic filters prove useful. One is a particle number concentration threshold where values above this threshold are flagged as unrealistic and contaminated. This threshold value should be high enough that any possible real aerosol events (e.g., long range transport of biomass smoke, volcanic or other aerosols) would not be flagged as local contamination. The 1-s data are monitored by the data acquisition system and if the number concentration value exceeds the threshold, the value for that minute is marked as contaminated. This threshold is currently set at $10,000 \text{ cm}^{-3}$ at SPO and is meant to capture obvious power plant, aircraft and other local aerosol plumes. A second filter is a derivative (i.e., rate of change) filter, which catches abrupt changes in the particle number concentration that would not be observed in aerosols transported long distances. If the 1-s particle concentration measurement exceeds the last 30-minute average by a factor of 4 or more, the entire minute is marked as contaminated. Finally, the data reviewer can make the subjective determination of whether the measurements are locally contaminated based on his/her experience with the historical data to minimize the chance that local emissions are identified as background aerosols. Manual quality control edits make up on average $\sim 6.5\%$ of the contamination edits identified at SPO, and often are necessary when winds are blowing from within the CAS but are very near the boundaries or when particle number concentrations are abnormally high (but do not exceed the automatic flagging threshold).

Table 4 also shows the percentage of aerosol data flagged as contaminated by the various automatic flagging criteria. The years 2003–2014 (the period for which we have 1-minute resolution aerosol data) are compared with the time period of 2006–2008, the period of peak human activity at

Table 4. Current NOAA automatic contamination flagging criteria.

Flag	Contamination Flag Criteria	Percentage of Data Removed (2003–2014)	Percentage of Data Removed (2006–2008)
Wind Direction	WD < 340° or WD > 110°	12.0%	14.1%
Wind Speed	WS < 0.5 m s ⁻¹	0.4%	0.4%
Particle Number Concentration	Conc > 10,000 cm ⁻³ and/or Conc > 4 × 0.5 h _{avg}	0.05%	0.05%

South Pole. The percentage of data flagged by the wind speed and particle concentration criteria is nearly identical in both ranges. A slightly higher percentage of observations was flagged for out of sector winds in the 2006–2008 period than in the longer record. These results do not necessarily support or refute the contention that the years 2006–2008 had more aerosol emissions based on more human activity. The percentage of data flagged by the particle concentration criteria depend strongly on whether the aerosol plumes directly hit the ARO, and this is in turn dependent on wind direction (not just winds being out of sector).

Fig. 4 shows that the winds at SPO have not changed considerably over the time period of our measurements; thus, it is reasonable to assume that the sampling of local contamination events has also not changed appreciably since the Bodhaine studies of the 1980's and 1990's. Increased local emissions in the mid-2000's suggest that if contamination identification was not handled well by our quality control procedures, enhanced aerosol loading would be observed in our clean data record during that period. No such enhancement is seen in Fig. 6, suggesting that increased amounts of locally-generated aerosol at SPO did not significantly contaminate the screened CAS measurements during the mid-2000's when the spike in human activity occurred. This also implies that the quality-control screening and editing procedures for measurements from wind directions falling outside of the CAS are robust.

Aside from the major long-term construction activities and population pulses at SPS, discrete events occur that are observed to contaminate the CAS air for relatively short periods (i.e., minutes to weeks) of time. These events have the potential to skew the CAS aerosol climatology and to affect long term trend analyses and the major types of events are reported here. Relating these events to possible contamination in the data record is necessary so that suspect data can be removed from the clean data archive.

Of historical importance is that the aircraft skiway at SPS physically extended into the CAS for decades. Occasionally, an LC-130 could just be getting off the snow at the end of the skiway and be in the CAS. Also, skiway grooming (heavy equipment) activity was thus required within the CAS for the skiway maintenance. This activity was noted in the CAS log, and this log was used to identify local contamination episodes. The skiway was "moved" in October 2008 when the skiway was extended south by ~1400 m and now ends at the main station (as shown in Fig. 1).

The most frequent type of discrete contamination event at SPO involves an aircraft flying at low altitude through the CAS. While this goes against normal NSF Clean Air Sector operating procedures, it happens with a typical frequency of several (i.e., 0–3) times per year. These violations can include approved flights to support deep field camps or traverses, Twin Otter aerial photography missions and LC-130 takeoffs that turn late or in the wrong direction (i.e., toward rather than away from the CAS). When a violation occurs, it is documented by SPS personnel and the time(s) of the violation are forwarded to the atmospheric monitoring groups so that data during the event can be inspected closely. These events are relatively easy to spot in the SPO aerosol data

record because the short-duration intense spikes in particle number concentration are easily detected by the particle concentration threshold and spike filters and all aerosol measurements at that time are flagged as contamination. Emissions from aircraft operating in the CAS are also often visible in the SPO radiation measurements (from contrails that move across the sky above ARO and cause short dips in the downwelling radiation values and/or in the images from the all-sky camera). The science technicians at SPO also generally note when this happens, if they happen to observe the event. Because these events are easily detected and flagged, we do not believe they have compromised the SPO aerosol clean data archive.

The other discrete type of event that can contaminate the CAS air is temporary construction or demolition activity. Generally, these actions are supposed to take place when the wind is blowing from the CAS so local aerosols do not impact the Clean Sector. Major efforts, however, are scheduled well in advance and people must be flown in for the job, and the schedule is difficult to change. The best example of this type of event is the sequence of explosions in summer 2010 required to demolish and collapse the original South Pole Station (referred to as 'Old Pole Station' and used from 1957 to 1974), which was completely buried under almost 10 m of snow. To accomplish the demolition, three explosions were triggered on 1, 4, and 7 December 2010, at 0316 UTC, 0300 UTC, and 0200 UTC, respectively. Times are accurate to the nearest minute and were verified using United States Geological Survey seismic data from the Antarctic QSPA site (~8 km from the South Pole). Winds were shifting in and out of sector during this period and the detonations all occurred when the winds were blowing to ARO from outside of the CAS. Fig. 8 is a map of the area with wind direction and speed (as measured at the ARO) at the time of each of the three blasts. The debris clouds should have roughly followed these vectors for at least several km since the lowest wind speed (during the second explosion) was 2.8 m s^{-1} (~10 km h^{-1}). Simple plume dispersion calculations suggest that the debris cloud from the third blast was almost certainly sampled as it passed by the ARO inlets, and the aerosols from the first blast may also have been directly sampled.

Fig. 9 is a photograph taken by NOAA personnel ~30 minutes after the blast on 4 December 2010 showing the debris cloud from the explosion heading to the northeast along the snow surface and entering the CAS to the NNW of the ARO. The view is toward grid direction east and the camera location was just north of the blast crater, which can be seen beyond the blue flags at the right. The ARO lies to the right of the flag line and out of the photograph.

One-minute resolution aerosol and wind data measured at ARO during the blasting period and the days immediately thereafter are shown in Fig. 10. The vertical red lines in all panels indicate the blast times. Periods when winds arrived at ARO from outside the CAS ($WD > 110$ and < 340 degrees, shown by the green lines in Fig. 10(d)) are indicated by the yellow shading. Much of the local aerosol contamination observed leading up to the first blast appears to have originated from the various dark sector buildings (which

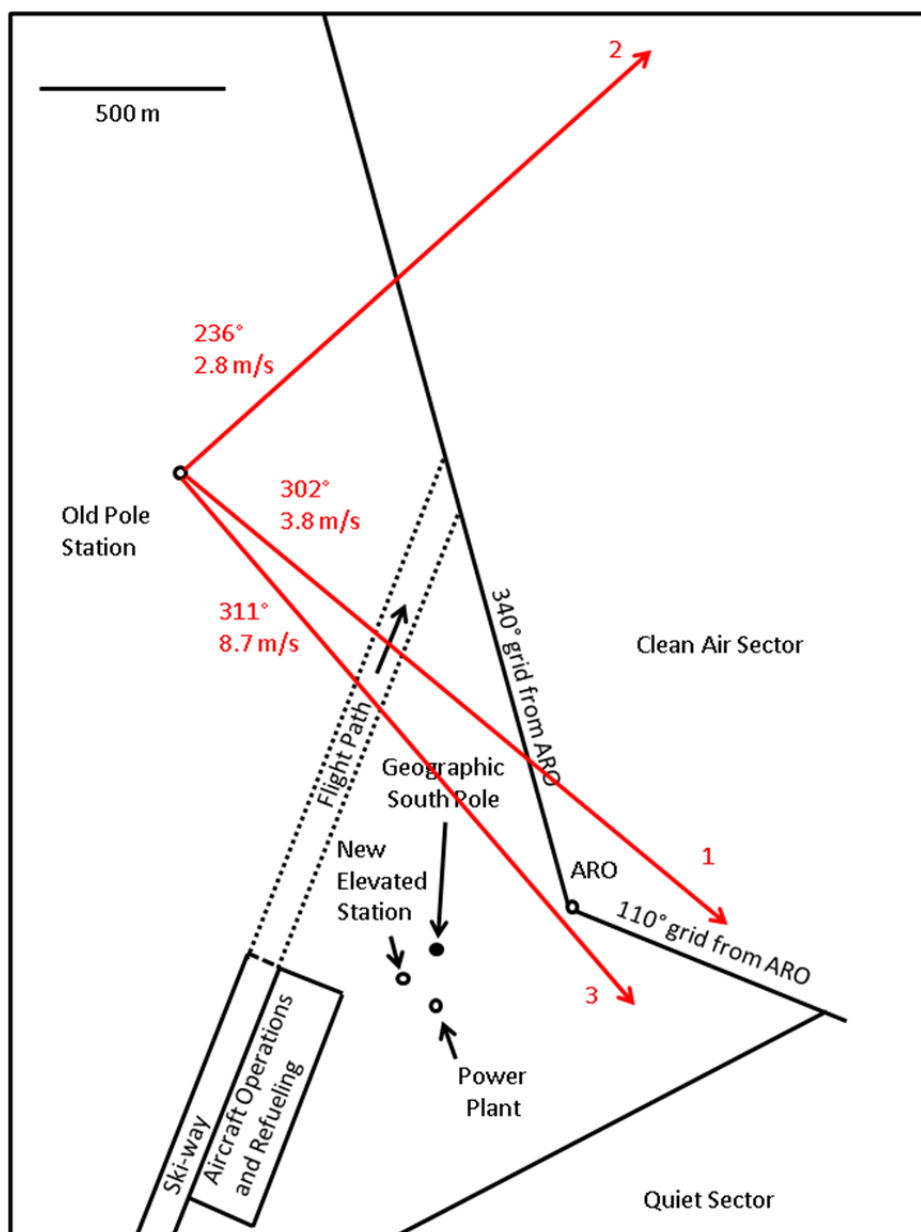


Fig. 8. Map showing the approximate tracks of the debris clouds immediately after each blast. Wind speed and direction are listed, as measured at the ARO, for the time of each blast.

are heated by fuel-burning furnaces) as well as the transportation and digging activity around the blasting site preparing for the explosion. For the second blast, the out-of-sector aerosol peaks up until about 1200 UTC on 3 December appear to come from the same area, whereas later on 3 December and up until the time of the blast on 4 December the largest peaks were probably from the power plant and main station facilities (possibly including planes). These same winds pushed the debris cloud from the second blast along the snow surface to the northeast and later to the north in the CAS. Wind speeds were relatively low during the second blast and particles settling out from this dust cloud would have deposited onto the snow surface in compass directions to the north of the ARO. For the last blast, aerosols could have come from activity around the

blast zone before the explosion, and blast particles in the debris cloud were likely sampled directly. The wind speeds were very high for this third blast, however ($> 30 \text{ km h}^{-1}$), so the debris cloud would have rapidly mixed with clean air and passed the ARO quickly.

It is evident that WD screening handles most of the contamination problem since all aerosol data during the yellow periods are flagged as contaminated and are not included in the clean data archive. In the days following the blast period, however, some anomalous aerosol measurements (i.e., roughly day-long enhancements in particle number concentration) were observed in air coming from the CAS. The median, 75th percentile and 95th percentile levels for all daily-average particle concentrations at SPO during December in the years 1979–2014 are 170,



Fig. 9. Photograph taken from just north of the 4 December 2010 blast crater (visible behind the blue flags), showing the debris cloud moving to the northeast and entering the CAS.

230, and 405 cm^{-3} , respectively. In the week after the final explosion, three particle concentration peaks were measured in the range of $800\text{--}1600\text{ cm}^{-3}$, and all seven daily averages from 9–15 December exceeded the 90th percentile of long-term, December daily-average values, with 5 days exceeding the 95th percentile level (shown by the green line in Fig. 10(a)). If these peaks were observed in the next day or so after the explosions it is possible that the suspended, re-circulated debris cloud was being sampled directly, but after 1–2 days the debris cloud would have been blown out of the CAS by the katabatic winds. Wind directions from the north to northeast (on 10 December, and subsequent days) correlate with abnormally high particle number concentrations, and WS shows a local maximum on 10 December. These broad peaks in particle number concentration could be from re-entrainment of particles from the snow surface from the second blast. We believe these particles were attached to fine snow/ice crystals on the surface and were re-suspended by wind activity. The crystals melt or evaporate in the aerosol inlet as they are brought into the ARO and the particles are left to be sampled and measured by the instruments. Since the SPO aerosol data following a series of huge particle generation events at SPS were suspect and well above normal values, the questionable aerosol measurements from the period following the blast were manually flagged as contaminated during data review. The period of manually flagged data (9–15 December) are shown by the purple line in Fig. 10(a). This is a conservative approach and requires some subjectivity, and some valid background data could possibly have been removed in this process.

This is preferable, however, to including contaminated data in the clean data archive. We believe that our methods in handling these discrete contamination events are robust and that these types of events at SPS have a minimal effect on the long-term SPO background aerosol record.

NOAA also monitors the concentrations of a large suite of greenhouse gases, halogenated gases and ozone at SPO. The majority of these trace gases are sampled periodically by flasks. Flasks are collected only when the winds have been consistently from the CAS and episodes of local contamination have not been reported. Because of the discrete nature of the flask measurements it is difficult to directly relate them to the aerosol measurements. Continuous measurements of selected gases are also made at SPO. These include the greenhouse gases CO_2 , N_2O , and SF_6 ; the halogenated compounds CFC-11, CFC-12, CCl_4 , CH_3CCl_3 , CFC-113, HCFC-142b, HCFC-22, Halon-1211, and CH_3Cl ; and O_3 . When episodes of local contamination are reported, observed or suspected, the continuous measurements are flagged similar to the aerosol measurements and these data are not included in the long-term, background data archives. More information on the NOAA measurements at SPO can be found at <http://www.esrl.noaa.gov/gmd/obop/spo/summary.html>.

CONCLUSIONS

The Atmospheric Research Observatory at the Amundsen-Scott South Pole station, a pristine and high elevation site located on the Antarctic Ice Plateau, is in a desirable

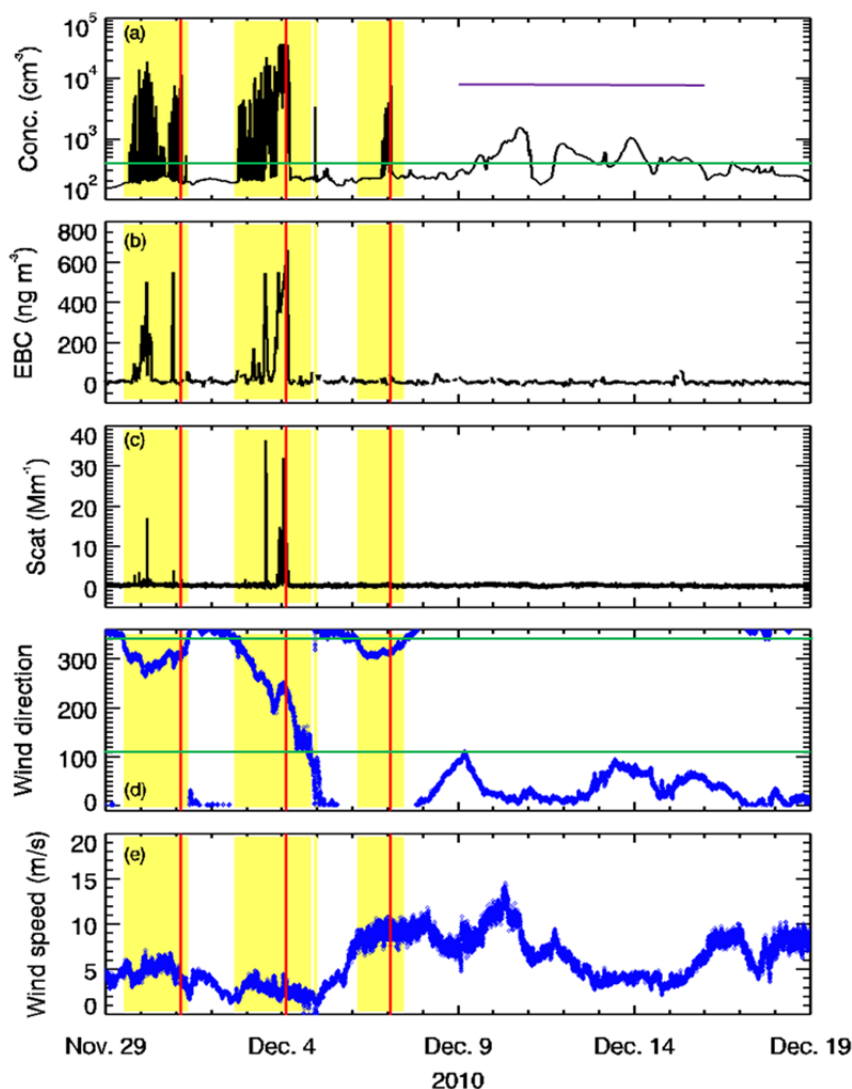


Fig. 10. Measurements made at ARO during the three Old Pole explosions (times shown by red lines) and immediately thereafter. Periods when winds were blowing from outside the CAS are shown in yellow. (a) Particle number concentration (cm^{-3}). Note the logarithmic scale, in contrast to the linear scale in Fig. 6(a). The green line shows the 95th percentile level of all December daily-average values in the historical record. The purple bar shows the data period that was considered anomalous and all aerosol data were flagged during this time. (b) Equivalent black carbon concentration (ng m^{-3}). (c) Aerosol light scattering coefficient (Mm^{-1} , 550 nm). (d) Wind direction (degrees). The green lines show the boundaries of the CAS. (e) Wind speed (m s^{-1}).

location for background atmospheric measurements. Climatologies of wind and aerosol measurements at the South Pole have been presented through 2014. The long-term wind data set indicates that winds at ARO blow from the Clean Air Sector an average of 88% of the time, and that this has not changed appreciably over the years. Even using the old, slightly larger definition of the CAS, this value remains below 90%. This is lower than the values of 95–98% reported in earlier papers.

Long-term time series and annual cycles of various aerosol properties have been presented for SPO. Analysis of the time series indicated that no significant trends were observed in any aerosol parameters except scattering Ångström exponent (550/700 nm), which had a statistically-significant downward trend of -0.02 yr^{-1} over the 36-year

record and suggests a gradually-increasing contribution to light scattering from larger particles. Analysis of the time series of data from the individual nephelometers showed no significant trends in Å_s , suggesting that all or part of the long-term trend might be driven by instrumental discrepancies. Differences in annual cycles among the aerosol properties suggest different sources/processes. For example, the light scattering measurements show highest values in the austral winter and spring and have been attributed to transport of marine aerosols from the southern ocean around Antarctica. In contrast, particle number concentration shows a broad minimum in the winter months which may be related to the lack of photochemical particle production and enhanced isolation of the Antarctic region due to the polar vortex.

Human activity markers were used to estimate the period

of peak anthropogenic emissions at SPO. This occurred in the mid- to late-2000's, after the South Pole Station Modernization project was completed and the IceCube SNO and South Pole Telescope projects were being built. Aerosol properties measured at ARO did not show increased aerosol amounts during this extended period of increased human activity, suggesting that NSF's Clean Air Sector management plan and our SPO local contamination screening procedures were working well. Discrete contamination events have also been identified in the data record and have been successfully handled. The indications are, based on winds and the aerosol measurements themselves, that local aerosol contamination of the CAS at SPO 1) is relatively infrequent, 2) has not changed significantly over the years, 3) can be handled effectively by the quality control procedures in place, and 4) has not affected the long term trends in background aerosol measurements to any appreciable extent.

This work illustrates the value in having data quality control procedures in place to identify and flag background aerosol data that are contaminated by local pollution or are otherwise anomalous. The possibility of recirculation of air masses requires a station to have more than simple wind monitoring to identify contaminated conditions. Particle number concentration is a sensitive and fast-response measurement that has been used successfully for automated and mentor-determined contamination.

ACKNOWLEDGMENTS

This study was supported by NOAA Climate Program Office's Atmospheric Chemistry, Carbon Cycle and Climate (AC4) program. The authors wish to thank the National Science Foundation and their Antarctic Support Contractors for the information on flights, fuel and population at South Pole. We also thank Johan Booth and the other NOAA science technicians at SPO who carefully conduct the measurements and keep accurate records of happenings at South Pole Station.

DISCLAIMER

Reference to any companies or specific commercial products does not constitute endorsement by the National Oceanic and Atmospheric Administration.

REFERENCES

- Anderson, T.L., and Ogren, J.A. (1998). Determining Aerosol Radiative Properties Using the TSI 3563 Integrating Nephelometer. *Aerosol Sci. Technol.* 29: 57–69.
- Asmi, A., Collaud Coen, M., Ogren, J.A., Andrews, E., Sheridan, P., Jefferson, A., Weingartner, E., Baltensperger, U., Bukowiecki, N., Lihavainen, H., Kivekäs, N., Asmi, E., Aalto, P.P., Kulmala, M., Wiedensohler, A., Birmili, W., Hamed, A., O'Dowd, C., Jennings, S.G., Weller, R., Flentje, H., Fjaeraa, A.M., Fiebig, M., Myhre, C.L., Hallar, A.G., Swietlicki, E., Kristensson, A., and Laj, P. (2013). Aerosol Decadal Trends – Part 2: In-situ Aerosol Particle Number Concentrations at GAW and Actris Stations. *Atmos. Chem. Phys.* 13: 895–916.
- Bodhaine, B.A. (1983). Aerosol Measurements at Four Background Sites. *J. Geophys. Res.* 88: 10753–10768.
- Bodhaine, B.A. (1995). Aerosol Absorption Measurements at Barrow, Mauna Loa and the South Pole. *J. Geophys. Res.* 100: 8967–8975.
- Bodhaine, B.A., and Murphy, M.E. (1980). Calibration of an Automatic Condensation Nuclei Counter at the South Pole. *J. Aerosol Sci.* 11: 305–312.
- Bodhaine, B.A., Deluisi, J.J., Harris, J.M., Houmère, P., and Bauman, S. (1986). Aerosol Measurements at the South Pole. *Tellus Ser. B* 38: 223–235.
- Carslaw, D.C. (2015). The Openair Manual - Open-source Tools for Analysing Air Pollution Data. Manual for Version 1.1-4, King's College London, pp. 162–170.
- Carslaw, D.C. and Ropkins, K. (2012). Openair - An R Package for Air Quality Data Analysis. *Environ. Modell. Software* 27–28: 52–61.
- CMDL (1992). In Summary Report #20, 1991. Ferguson, E.E. (Ed.), Climate Monitoring and Diagnostics Laboratory, Boulder, pp. 52–57.
- CMDL (1994). In Summary Report #22, 1993. Peterson, J.T. (Ed.), Climate Monitoring and Diagnostics Laboratory, Boulder, pp. 60–65.
- CMDL (1998). In Summary Report #24, 1996–1997. Hofmann, D.J. and Peterson, J.T. (Eds.), Climate Monitoring and Diagnostics Laboratory, Boulder, pp. 14–29.
- Collaud Coen, M., Andrews, E., Asmi, A., Baltensperger, U., Bukowiecki, N., Day, D., Fiebig, M., Fjaeraa, A.M., Flentje, H., Hyvärinen, A., Jefferson, A., Jennings, S.G., Kouvarakis, G., Lihavainen, H., Lund Myhre, C., Malm, W.C., Mihapopoulos, N., Molenaar, J.V., O'Dowd, C., Ogren, J.A., Schichtel, B.A., Sheridan, P., Virkkula, A., Weingartner, E., Weller, R., and Laj, P. (2013). Aerosol Decadal Trends – Part 1: In-situ Optical Measurements at GAW and IMPROVE Stations. *Atmos. Chem. Phys.* 13: 869–894.
- Collaud Coen, M., Weingartner, E., Apituley, A., Ceburnis, D., Fierz-Schmidhauser, R., Flentje, H., Henzing, J.S., Jennings, S.G., Moerman, M., Petzold, A., Schmid, O., Baltensperger, U. (2010). Minimizing Light Absorption Measurement Artifacts of the Aethalometer: Evaluation of Five Correction Algorithms. *Atmos. Meas. Tech.* 3: 457–474.
- Collaud Coen, M., Weingartner, E., Nyeki, S., Cozic, J., Henning, S., Verheggen, B., Gehrig, R. and Baltensperger, U. (2007). Long-term Trend Analysis of Aerosol Variables at the High Alpine Site Jungfraujoch. *J. Geophys. Res.* 112: D13213, doi: 10.1029/2006JD007995.
- Delene, D.J. and Ogren, J.A. (2002). Variability of Aerosol Optical Properties at Four North American Surface Monitoring Sites. *J. Atmos. Sci.* 59: 1135–1150.
- ESRL Global Monitoring Division - Nephelometer Operations Manual, <http://www.esrl.noaa.gov/gmd/obop/spo/observatory.html>, Last Access: 31 August 2015.
- ESRL Global Monitoring Division - South Pole Observatory, <http://www.esrl.noaa.gov/gmd/obop/spo/observatory.ht>

- ml, Last Access: 31 August 2015.
- ESRL Global Monitoring Division - SPO Measurements Summary, <http://www.esrl.noaa.gov/gmd/obop/spo/summary.html>, Last Access: 31 August 2015.
- Fiebig, M., Hirdman, D., Lunder, C.R., Ogren, J.A., Solberg, S., Stohl, A. and Thompson, R.L. (2014). Annual Cycle of Antarctic Baseline Aerosol: Controlled by Photooxidation-limited Aerosol Formation. *Atmos. Chem. Phys.* 14: 3083–3093.
- Fletcher, R.A., Mulholland, G.W., Winchester, M.R., King, R.L. and Klinedinst, D.B. (2009). Calibration of a Condensation Particle Counter Using a NIST Traceable Method. *Aerosol Sci. Technol.* 43: 425–441.
- Hansen, A.D.A. (2003a). In *The Aethalometer*, v. 2003.04, Magee Scientific Company, Berkeley, California, p. 24.
- Hansen, A.D.A. (2003b). Measurement of Combustion Effluent Aerosols from the South Pole Station. Final Report to National Science Foundation, Project S-314.
- Hansen, A.D.A., Bodhaine, B.A., Dutton, E.G. and Schnell, R.C. (1988). Aerosol Black Carbon Measurements at the South Pole: Initial Results, 1986–1987. *Geophys. Res. Lett.* 15: 1193–1196.
- Harris, J.M. (1992). An Analysis of 5-Day Midtropospheric Flow Patterns for the South Pole: 1985–1989. *Tellus Ser. B* 44: 409–421.
- Hermann, M., Wehner, B., Bischof, O., Han, H.-S., Krinke, T., Liu, W., Zerrath, A. and Wiedensohler, A. (2007). Particle Counting Efficiencies of New TSI Condensation Particle Counters. *J. Aerosol Sci.* 38: 674–682.
- IceCube Neutrino Observatory, <https://icecube.wisc.edu>, Last Access: 31 August 2015.
- Liu, W., Kaufman, S.L., Osmondson, B.L., Sem, G.J., Quant, F.R. and Oberreit, D.R. (2006). Water-Based Condensation Particle Counters for Environmental Monitoring of Ultrafine Particles. *J. Air Waste Manage. Assoc.* 56: 444–455.
- Management Plan for Antarctic Specially Managed Area No 5, http://www.ats.aq/documents/recatt/Att357_e.pdf, Last Access: 31 August 2015.
- National Science Foundation – Antarctic Polar Vortex, <https://www.nsf.gov/about/history/nsf0050/arctic/ozone.htm>, Last Access 31 August 2015.
- National Science Foundation Antarctic Support Contractors (2015). Personal Communications.
- Parungo, F., Bodhaine, B. and Bortniak, J. (1981). Seasonal Variation in Antarctic Aerosol. *J. Aerosol Sci.* 12: 491–504.
- Petzold, A., Ogren, J.A., Fiebig, M., Laj, P., Li, S.M., Baltensperger, U., Holzer-Popp, T., Kinne, S., Pappalardo, G., Sugimoto, N., Wehrli, C., Wiedensohler, A. and Zhang, X.Y. (2013). Recommendations for Reporting “Black Carbon” Measurements. *Atmos. Chem. Phys.* 13: 8365–8379.
- Pollak, L.W. and Metnieks, A.L. (1960). Intrinsic Calibration of the Photoelectric Nucleus Counter Model 1957, With Convergent Light Beam. Tech. Note 9, Contract AF61 (052)-26, School of Cosmic Physics, Dublin Institute for Advanced Studies.
- Sheridan, P.J., Delene, D.J. and Ogren, J.A. (2001). Four Years of Continuous Surface Aerosol Measurements from the Department of Energy’s Atmospheric Radiation Measurement Program Southern Great Plains Cloud and Radiation Testbed Site. *J. Geophys. Res.* 106: 20735–20747.
- Sherman, J.P., Sheridan, P.J., Ogren, J.A., Andrews, E., Hageman, D., Schmeisser, L., Jefferson, A. and Sharma, S. (2015). A Multi-Year Study of Lower Tropospheric Aerosol Variability and Systematic Relationships From Four North American Regions. *Atmos. Chem. Phys.* 15: 12487–12517, doi: 10.5194/acp-15-12487-2015.
- Sinclair, D. (1984). Intrinsic Calibration of the Pollak Counter – A Revision. *Aerosol Sci. Technol.* 3: 125–134.
- Spracklen, D.V., Carslaw, K.S., Merikanto, J., Mann, G.W., Reddington, C.L., Pickering, S., Ogren, J.A., Andrews, E., Baltensperger, U., Weingartner, E., Boy, M., Kulmala, M., Laakso, L., Lihavainen, H., Kivekas, N., Komppula, M., Mihalopoulos, N., Kouvarakis, G., Jennings, S.G., O’Dowd, C., Birmili, W., Wiedensohler, A., Weller, R., Gras, J., Laj, P., Sellegri, K., Bonn, B., Krejci, R., Laaksonen, A., Hamed, A., Minikin, A., Harrison, R.M., Talbot, R. and Sun, J. (2010). Explaining Global Surface Aerosol Number Concentrations in Terms of Primary Emissions and Particle Formation. *Atmos. Chem. Phys.* 10: 4775–4793.
- Warren, S.G. and Clarke, A.D. (1990). Soot in the Atmosphere and Snow Surface of Antarctica. *J. Geophys. Res.* 95: 1811–1816.
- Weingartner, E., Saathoff, H., Schnaiter, M., Streit, N., Bitnar, B. and Baltensperger, U. (2003). Absorption of Light by Soot Particles: Determination of the Absorption Coefficient by Means of Aethalometers. *J. Aerosol Sci.* 34: 1445–1463.
- Yu, F., Luo, G., Turco, R.P., Ogren, J.A. and Yantosca, R.M. (2012). Decreasing Particle Number Concentrations in a Warming Atmosphere and Implications. *Atmos. Chem. Phys.* 12: 2399–2408.

Received for review, May 22, 2015

Revised, August 31, 2015

Accepted, September 8, 2015